

Pure Nanoporous Gold Powder: Synthesis and Catalytic Properties

Thierry Déronzier,[†] Franck Morfin,[†] Laurence Massin,[†] Marc Lomello,[‡] and Jean-Luc Rousset^{*,†}[†]IRCELYON, UMR 5256, CNRS, Université de Lyon, 69626 Villeurbanne Cedex, France[‡]SYMME, Polytech' Savoie, B.P. 80439, 74944 Annecy le Vieux Cedex, France**S** Supporting Information**KEYWORDS:** catalysis, gold, nanoporous, CO oxidation, H₂ oxidation

Among the interests of the scientific community in developing nanoporous systems for their potential applications in the separation of large molecules, sensors, catalysis, and drug delivery, a great deal of effort has specifically been devoted to the synthesis of pure nanoporous gold. From a fundamental point of view, these systems are perfectly adapted to the study of the intrinsic activity of the metallic phase in the catalytic process, owing to the absence of a support. Regarding gold, as pointed out first by Haruta, this current interest^{1–7} is governed by a fundamental question of the catalysis by gold: Is unsupported gold catalytically active?^{8,9} This question follows extensive research in the field of catalysis by supported gold to account for its high activity toward several important oxidation reactions. Among these, CO oxidation,¹⁰ the water gas shift reaction,¹¹ the epoxidation of propylene,¹² and the direct synthesis of H₂O₂ from H₂ and O₂¹³ are all known to be catalyzed by gold.

Despite these efforts, there is still continuous debate on the size, charge state and support effects, the nature of the active site, and especially in what way and on which site O₂ is activated. The general opinion is that neutral gold clusters alone cannot activate the O–O bond without some influence from the substrate such as charge-transfer processes or specific interfacial sites. Here, we report on the synthesis and CO oxidation behavior of extremely pure gold nanofoam material.

Existing methods up to now have failed to produce pure nanoporous gold. In particular, the dealloying of gold–silver or gold–copper alloys has been the most widely used. This dealloying is a common corrosion process during which an alloy is “parted” by the selective dissolution of the electrochemically more active elements.¹⁴ This process results in the formation of a nanoporous sponge composed almost entirely of the more noble alloy constituents that exhibits skeletal morphology with tunable pore and ligament sizes of nanometer level. Several groups have shown that such nanoporous gold exhibits very high activity for CO oxidation at low temperature. Some of these groups have noted that residual impurities should play a role in the activation of O₂. Moreover a consensus seems to emerge that the high activity observed on these systems toward CO oxidation could be ascribed to the presence of a large (few atomic %) superficial amount of these residual impurities.^{5,6} Baumer and co-workers have, moreover, published a paper entitled “Nanoporous Au: An unsupported pure gold catalyst?”⁹ and their answer is “no”. Hence, the question asked by Haruta remains unanswered until now. To

demonstrate unequivocally whether gold alone is able to efficiently oxidize CO requires the synthesis of high surface area unsupported gold material without any superficial impurities.

The nanoporous gold used here is synthesized by a new two-step method. At first, an intimate mixture of a skeletal gold structure with ZrO₂ nanoparticles is obtained by mild oxidation of an Au_{0.5}Zr_{0.5} intermetallic alloy.¹⁵ The zirconia is then selectively dissolved in fluorhydric acid. The resulting gold system is a micrometric powder composed of grains whose sizes are between a few μm and 200 μm. Each grain resembles a nanoporous sponge, as shown in Figure 1.

A specific surface area of 9 m²/g was found for this material by determining nitrogen adsorption isotherms at 77 K (the data were processed using the Brunauer, Emmet, and Teller (BET) method).

Before the leaching of zirconia, the size of the gold crystallites estimated from the broadening of X-ray diffraction peaks by fitting the whole pattern using the scherrer method is found to be about 7 nm.¹⁵ The diffraction pattern of the sample revealed the formation of larger Au crystallites (20 nm) after selective dissolution of the ZrO₂.

SEM, BET, and XRD analyses therefore show that the systems we obtain have superficial structures identical to that reported for typical npAu samples made by dealloying methods.

The sample was then analyzed by inductively coupled plasma optical emission spectroscopy (ICP-OES), and a residual Zr bulk content of 0.03% was determined. To check for a distinct amount of Zr in the surface region and/or the presence of fluorine, X-ray photoemission spectroscopy (XPS) was further conducted. Because both Zr impurity measured by ICP and fluorine are absent from XPS spectra and thus from the gold surface, they should therefore not contribute to the observed catalytic behavior.

This material was tested in three catalytic reactions, the oxidation of CO, the selective oxidation of CO in the presence of H₂, and the oxidation of H₂, all using the same protocol. Only the incoming gas mixture was changed from one reaction to the other. The catalytic tests were carried out under atmospheric pressure in a flow reactor at temperatures from 25 to 150 °C using 50 N ml·min⁻¹ total flow of reactants in helium carrier gas. In the absence of H₂, CO oxidation proceeds

Received: July 22, 2011

Revised: November 8, 2011

Published: November 23, 2011



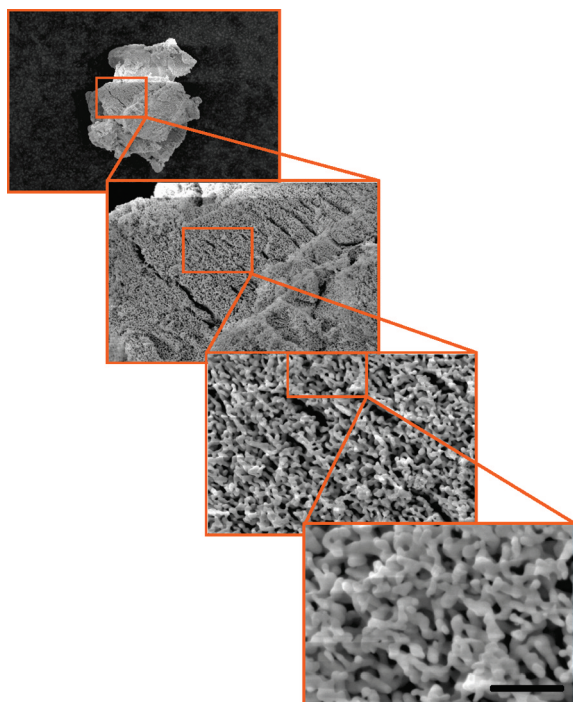


Figure 1. SEM images of a typical grain of nanoporous gold powder manufactured by a two-step process. At first the oxidation (in air at RT) of a roughly ground $\text{Au}_{0.5}\text{Zr}_{0.5}$ alloy lead to the formation of a powder made up of an intimate mixture of nanostructured gold and zirconia. This first step is followed by the selective dissolution of zirconia in fluorhydric acid. The material obtained is homogeneous and its surface area is $9\text{ m}^2\text{g}^{-1}$. Scale bar is 500 nm.

through the difficult O_2 dissociation step and the oxidation rate observed over our nanoporous gold is very low (Figure 2).

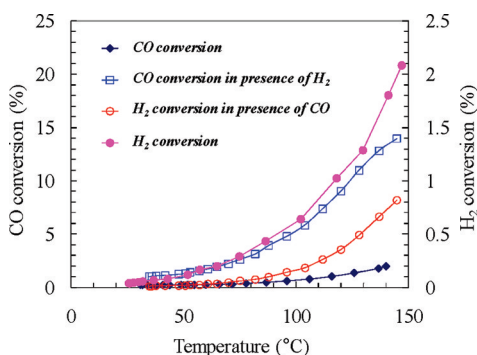


Figure 2. CO and H_2 conversion as a function of temperature. The reactant flow consisted of a mixture of 2% CO + 2% O_2 + 96% He for the oxidation of CO; 2% CO + 2% O_2 + 48% H_2 + 48% He for the preferential oxidation of CO (PrOx) and 48% H_2 + 2% O_2 + 50% He for the oxidation of H_2 (all percentages are vol %).

CO conversion reaches only 2% at 140 °C. The corresponding calculated rate per surface atom (TON) is at least about 3 orders of magnitude lower than that observed on other nanoporous gold containing residual silver or copper.^{3,5,7} This TON is also very small, as compared to that of oxide-supported gold nanoparticles (for example Au/ TiO_2 or Au/ Fe_2O_3 reference catalysts). To confirm that there are no artifacts associated with this surprising result, we synthesized a sample structurally similar to our npAu but containing

2 atom % silver. The reactivity of this sample was then analyzed in the same conditions as those used for the pure npAu. The activity of this AuAg sample toward CO oxidation was found to be some orders of magnitude higher than that observed on our pure nanoporous gold thus showing unambiguously that the high activity reported up to now for nanoporous gold is related to the presence of residual silver.

In the course of our investigation of PrOx reaction on gold supported catalysts, we have focused on the effect of H_2 addition on CO oxidation. We have shown that the CO oxidation pathway is strongly modified in the presence of H_2 .^{16,17} Indeed, even a low H_2 amount added to a CO + O_2 feed appears to accelerate CO oxidation. Here, the introduction of hydrogen in the reactant feed also results in an increase of the CO oxidation rate, as observed over alumina supported gold catalysts.¹⁶ For these materials, hydrogen has been reported to activate O_2 apparently in the same manner as reducible oxides.¹⁷ In the present case, the PrOx reaction proceeds with complete selectivity toward CO at low temperature (no water is formed up to 60 °C). This shows that the O_2 activation step, which is rate-determining in CO– O_2 mixtures, is facilitated in PrOx mixtures whether the gold catalyst is supported or not. As the temperature increases, hydrogen starts to be oxidized to water, thus competing with CO for reaction with oxygen. From our previous work on CO oxidation¹⁸ and PrOx,^{16,17} it has become obvious that gold-catalyzed CO oxidation does not proceed in the same way depending on whether hydrogen is present in the feed or not. The presence of hydrogen accelerates CO oxidation, which suggests a change in the reactive species, leading to specific mechanism and kinetics. The extent of this promotion is larger when the catalyst is highly active for hydrogen oxidation to water. We have previously shown that water is not the relevant intermediate and have suggested that the gold–hydroperoxy (Au–OOH) species may be the critical oxidizing one.^{16,17}

A comprehensive mechanism of this promotion has been suggested.¹⁷ In this scheme, molecularly adsorbed O_2 is activated on Au by reaction with H_2 , to form $\text{OOH}^{(a)}$ and $\text{H}^{(a)}$ species where (a) refers to the adsorbed species. Actually, these highly oxidative intermediates such as OH and OOH on Au catalysts under PrOx conditions have already been identified earlier by means of high-resolution scanning tunneling microscopy (STM),²¹ inelastic neutron scattering,²² and UV–vis/X-ray spectroscopy.²³

This mechanism, as shown in Figure 3, does not require O_2 dissociation on Au, which is known to be a highly activated step.^{19,20}

Hydrogen dissociation is easier than O_2 dissociation (and promoted by O_2) and $\text{H}^{(a)}$ stabilizes O_2 adsorption, thus favoring the formation of OOH species on gold.²⁰

Besides, activation of O_2 through the formation and dissociation of peroxide OOH has also been invoked in the selective oxidation of alcohols in aqueous phase over gold catalysts.²⁴ Hence, introduction of H_2 in a CO + O_2 mixture opens channels that cause O_2 to hydrogenate and dissociate easily providing O for CO oxidation. This means that superficial $\text{CO}^{(a)}$ and $\text{OOH}^{(a)}$ then convert to CO_2 and $\text{OH}^{(a)}$; next, $\text{OH}^{(a)}$ reacts with $\text{CO}^{(a)}$ to produce CO_2 and $\text{H}^{(a)}$. The cycle is closed when the two $\text{H}^{(a)}$ recombine into H_2 or react with O_2 molecules to form new $\text{OOH}^{(a)}$ species. Density-functional theory (DFT) calculations provide stability assessments and structural pictures for the various Au– H_xO_y species.^{19,20,24,25} However, the participation of OOH species

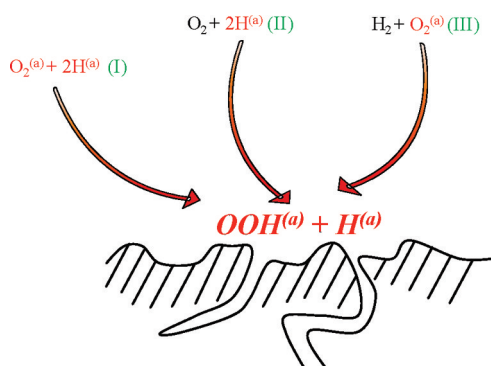


Figure 3. Schematic representation of the H-assisted O_2 activation at low temperature. In this temperature range, the PrOx reaction proceeds with complete selectivity toward CO_2 . Three mechanisms could lead to OOH intermediate species without requiring O_2 dissociation. (II) and (III) processes are representative of predicted Eley–Rideal mechanism.^{19,20}

in the reaction pathway was never verified, implying that other reasons for CO oxidation enhancement such as coadsorbate induced modifications of the reaction barriers could be equally possible.

To our knowledge, the work reported here concerns the first synthesis of extremely pure nanoporous gold. Investigation of its intrinsic catalytic properties revealed a very poor activity toward CO oxidation. This contrast with the high activity reported up to now on nearly identical materials, but which contain superficial impurities resulting from the manufacturing processes, strongly suggests that this high activity is primarily related to the presence of these residual surface impurities. The present study also shows that a new way of CO oxidation is opened up in the presence of hydrogen. However, even with hydrogen, our nanoporous gold is found to be less efficient than the oxide-supported ones for activating oxygen. Because gold catalyzed CO oxidation in the presence of H_2 and H_2 oxidation are basically independent of the supports,^{16,17} the small activity observed is probably related to a lower concentration of low-coordination active sites present at the surface, as compared to small gold particles.

■ ASSOCIATED CONTENT

📄 Supporting Information

Materials and methods for syntheses and experiments. This material is available free of charge via the Internet at <http://pubs.acs.org/>.

■ AUTHOR INFORMATION

Corresponding Author

*Tel.: (+33) 04 72 44 54 34. Fax: (+33) 04 72 44 53 99. E-mail: jean-luc.rousset@ircelyon.univ-lyon1.fr.

■ ACKNOWLEDGMENTS

The authors thank the French Research Agency for funding Project No. ANR-09-NANO-015 (PEPS). We also gratefully acknowledge Dr. N. S. Prakash for a critical reading of the manuscript.

■ REFERENCES

(1) Wittstock, A.; Zielasek, V.; Biener, J.; Friend, C. M.; Bäumer, M. *Science* **2010**, *327*, 319–322.

(2) Yin, H.; Zhou, C.; Xu, C.; Liu, P.; Xu, X.; Ding, Y. *J. Phys. Chem. C* **2008**, *112*, 9673–9678.

(3) Kameoka, S.; Tsai, A. P. *Catal. Lett.* **2008**, *121*, 337–341.

(4) Biener, J.; Wittstock, A.; Zepeda-Ruiz, L. A.; Biener, M. M.; Zielasek, V.; Kramer, D.; Viswanath, R. N.; Weissmüller, J.; Bäumer, M.; Hamza, A. V. *Nat. Mater.* **2009**, *8*, 47–51.

(5) Xu, C.; Xu, X.; Su, J.; Ding, Y. *J. Catal.* **2007**, *252*, 243–248.

(6) Xu, C.; Su, J.; Xu, X.; Liu, P.; Zhao, H.; Tian, F.; Ding, Y. *J. Am. Chem. Soc.* **2007**, *129*, 42–43.

(7) Zielasek, V.; Jürgens, B.; Schulz, C.; Biener, J.; Biener, M. M.; Hamza, A. V.; Baumer, M. *Angew. Chem. Int. Ed.* **2006**, *45*, 8241–8244.

(8) Haruta, M. *ChemPhysChem* **2007**, *8*, 1911–1913.

(9) Wittstock, A.; Neumann, B.; Schaefer, A.; Dumbuya, K.; Kübel, C.; Biener, M. M.; Zielasek, V.; Steinrück, H. P.; Gottfried, J. M.; Biener, J.; Hamza, A.; Bäumer, M. *J. Phys. Chem. C* **2009**, *113*, 5593–5600.

(10) Bond, G. C.; Thompson, D. T. *Catal. Rev. Sci. Eng.* **1999**, *41*, 319.

(11) Andreeva, D.; Idakiev, V.; Tabakova, T.; Ilieva, L.; Falaras, P.; Bourlinos, A.; Travlos, A. *Catal. Today* **2002**, *72*, 51.

(12) Sinha, A. K.; Seelan, S.; Akita, T.; Tsubota, S.; Haruta, M. *Appl. Catal., A* **2003**, *240*, 243.

(13) Landon, P.; Collier, P. J.; Carley, A. F.; Chadwick, D.; Papworth, A. J.; Burrows, A.; Kiely, C. J.; Hutchings, G. J. *Phys. Chem. Chem. Phys.* **2003**, *5*, 1917.

(14) Erlebacher, J.; Aziz, M. J.; Karma, A.; Dimitrov, N.; Sieradzki, K. *Nature* **2001**, *410*, 450–453.

(15) Lomello-Tafin, M.; Ait Chaou, A.; Morfin, F.; Caps, V.; Rousset, J. L. *Chem. Commun.* **2005**, *3*, 388–390.

(16) Rossignol, C.; Arrii, S.; Morfin, F.; Piccolo, L.; Caps, V.; Rousset, J. L. *J. Catal.* **2005**, *230*, 476–483.

(17) Quinet, E.; Piccolo, L.; Morfin, F.; Avenier, P.; Diehl, F.; Caps, V.; Rousset, J. L. *J. Catal.* **2009**, *268*, 384–389.

(18) Arrii, S.; Morfin, F.; Renouprez, A. J.; Rousset, J. L. *J. Am. Chem. Soc.* **2004**, *126*, 1199–1205.

(19) Barton, D. G.; Podkolzin, S. G. *J. Phys. Chem. B* **2005**, *109*, 2262–2274.

(20) Barrio, L.; Liu, P.; Rodriguez, A.; Campos-Martin, J. M.; Fierro, J. L. G. *J. Phys. Chem. C* **2007**, *111*, 19001–19008.

(21) Matthiesen, J.; Wendt, S.; Hansen, J.; Madsen, G. K. H.; Lira, E.; Galliker, P.; Vestergaard, E. K.; Schaub, R.; Lægsgaard, E.; Hammer, B.; Besenbacher, F. *ACS Nano* **2009**, *3*, 517–526.

(22) Sivadinarayana, C.; Choudhary, T. V.; Daemen, L. L.; Eckert, J.; Goodman, D. W. *J. Am. Chem. Soc.* **2004**, *126*, 38–39.

(23) Bravo-Surez, J. J.; Bando, K. K.; Lu, J.; Haruta, M.; Fujitani, T.; Oyama, T. *J. Phys. Chem. C* **2008**, *112*, 1115–1123.

(24) Zope, B. N.; Hibbitts, D. D.; Neurock, M.; Davis, R. J. *Science* **2010**, *330*, 74–78.

(25) Bongiorno, A.; Landman, U. *Phys. Rev. Lett.* **2005**, *95*, 106102.